Optical Tweezers

Experiment OT - sjh,rd

University of Florida — Department of Physics
PHY4803L — Advanced Physics Laboratory

Objective

An optical tweezers apparatus uses a tightly focused laser to generate a trapping force that can capture and move small particles under a microscope. Because it can precisely and non-destructively manipulate objects such as individual cells and their internal components, the optical tweezers is extremely useful in biological physics research. In this experiment the student will use optical tweezers to trap small silica spheres immersed in water. By analyzing the dynamics of particles held in the trap, including the frequency spectrum of their Brownian motion and their response to hydrodynamic drag, the student will characterize the physical parameters of the optical trap with high precision. The apparatus can then be used to measure a microscopic biological force, such as the force that propels a swimming bacterium or the force generated by a transport motor operating inside a plant cell.

References

D.C. Appleyard *et al.*, *Optical trapping for undergraduates*, Am. J. Phys. **75** 5-14 (2007).

A. Ashkin, *Acceleration and Trapping of Particles by Radiation Pressure*, Phys. Rev. Lett. **24** 156-159 (1970).

K. Berg-Sorensen and H.Flyvbjerg, *Power spectrum analysis for optical tweezers*, Rev. Sci. Instr. **75** 594-612 (2004).

S. Chattopadhyay, R. Moldovan, C. Yeung, X.L. Wu, *Swimming efficiency of bacterium Escherichiacoli*, Proc. Nat. Acad. Sci. USA **103** 13712-13717 (2006).

Daniel T. Gillespie *The mathematics of Brownian motion and Johnson noise*, Amer. J. of Phys. **64** 225 (1996).

Daniel T. Gillespie *Fluctuation and dissipation in Brownian motion*, Amer. J. of Phys. **61** 1077 (1993).

S.F. Tolic-Norrelykke *et al.*, *Calibration of optical tweezers with positional detection in the back focal plane*, Rev. Sci. Instr. **77** 103101 (2006).

Introduction

The key idea of optical trapping is that a laser beam brought to a sharp focus generates a restoring force that can pull particles into that focus. Arthur Ashkin demonstrated the principle in 1970 and reported on a working apparatus in 1986. The term optical trapping often refers to laser-based methods for holding neutral atoms in high vacuum, while the term optical tweezers (or laser tweezers) typically refers to the application studied in this

experiment: A microscope is used to bring a laser beam to a sharp focus inside an aqueous sample, such that microscopic, non-absorbing particles such as small beads or individual cells can become trapped at the beam focus. Optical tweezers have had a dramatic impact on the field of biological physics, as they allow experimenters to measure non-destructively and with high precision the tiny forces generated by individual cells and biomolecules. This includes propulsive forces generated by swimming bacteria, elastic forces generated by deformation of biomolecules, and the forces generated by processive enzyme motors operating within a cell. Experimenting with an apparatus capable of capturing, transporting, and manipulating individual cells and organelles provides an intriguing introduction to the world of biological physics.

A photon of wavelength λ and frequency $f = c/\lambda$ carries an energy $E = hf$ and a momentum of magnitude $p = h/\lambda$ in the direction of propagation.[1] Note that our laser power—around 100 mW—focused down to a few square microns, imply laser intensities around 10^7 W/cm^2 at the beam focus. Particles that absorb more than a tiny fraction of the incident beam will absorb a large amount of energy relative to their volume rather quickly. In fact, light-absorbing particles can be quite rapidly vaporized (opticuted) by the trapping laser. (Incidentally, your retina contains many such particles - see *Laser Safety* below). While the scatterer and surrounding fluid always absorbs some energy, our infrared laser wavelength ($\lambda = 975$ nm) is specifically chosen because it is where absorption in water and most biological samples is lowest. The absorption rate is also near a minimum for the silica spheres you will study. You should keep an eye out for evidence of heating in your samples, but because of the relatively low absorption rate and because the particle has good thermal conductance with the surrounding water, effects of heating should be modest.

The laser force arises almost entirely from the elastic scattering of laser photons by the particle whereby the particle alters the direction of the photon momentum without absorbing any of its energy. The laser force is typically decomposed into two components: (1) a scattering force proportional to the laser intensity and (2) a gradient force proportional to the gradient of laser intensity. The scattering force is in the direction of the laser beam, while the gradient force depends on the spatial dependence of the laser intensity and near the focus provides the Hooke's law force responsible for trapping the particle. The origin of both forces is similar: the particle elastically scatters a photon and alters its momentum. Momentum conservation implies that the scattered photon imparts an equal and opposite momentum change to the particle. The net force on the particle is a vector equal and opposite the net rate of change of momentum of the laser photons.

The theory and practice of laser tweezers are highly developed and numerous excellent reviews, tutorials, examples, and other resources on the subject are available[2]. For particles with diameters d large compared to λ, a ray optics model gives a good description of the physics that generates the force due to the laser. Reflection and refraction of the rays at the surface of the sphere alter the direction of the rays and thus the momentum they carry. The laser force is the cumulative effect from all the scattered photons. For smaller particles of diameter $d \ll \lambda$, Rayleigh scattering describes the interaction: The particle acts as a point dipole, scattering the incident beam in a spatially dependent fashion that depends on the

[1] h = Planck's constant, c = speed of light.

[2] Google: optical tweezers

location of the particle, leading to a trapping force on the particle.

The center of the trap will be taken as ($\mathbf{r} = 0$). For any small displacement (any direction) away from the trap center the particle is subject to a Hooke's law restoring force, i.e., proportional to and opposite the displacement. Detailed calculations show that the force constants are sensitive to the shape and intensity of the laser field, the size and shape of the trapped particle, and the optical properties of the particle and surrounding fluid. Consequently the Hooke's law force is difficult to predict. Furthermore, our apparatus operates in an intermediate regime of particle sizes where neither the ray optics nor Rayleigh models are truly appropriate. The diameter d of the silica spheres (SiO_2) range in size from 0.5-5 μm. Thus with the laser wavelength of $\lambda = 975$ nm, we have $d \sim \lambda$. Fortunately we do not need to calculate or predict the Hooke's law force constants. We only need to understand their physical origin. In this lab you will learn how to calibrate the trap by measuring the force constants indirectly on a trapped particle in a fluid. With an accurate force calibration method at hand, one can measure and explore biomolecular forces quantitatively.

Physics of the trapped particle

The design, operation, and calibration of our laser tweezers draws on principles of optics, mechanics and statistical physics. We begin with an overview of the physics that is relevant to generating and calibrating the trap. We then describe the design of the apparatus and the procedure for calibration.

Consider the motion and forces in terms of their components. Suppose the laser beam propagates in the $+z$ direction, so the x and y coordinates describe the horizontal plane – perpendicular to the beam propagation direction. Because the laser beam and focusing optics are cylindrically symmetric around the z-axis, the trap has the same properties in the x-direction as in the y-direction. We need only consider the equations for the x motion of the particle, and a similar set of equations will describe the motion in the y-direction. However the trapping force that acts along the z direction is different than for x and y, as the laser intensity in the focal region is clearly not a spherically symmetric pattern. The width of the beam focus in its radial (xy) dimension is very narrow. It is limited by wave diffraction to roughly one wavelength ($\lambda \sim 1\mu$m), whereas this is not the case in z. Hence the restoring force in z is not necessarily as strong as in xy. If the beam is not very tightly focused along the z-direction, the trapping force in the z-direction may be too weak. If the focal "cone" has too shallow an angle (technically, a large f-number or small *numerical aperture*), particles may be trapped in the xy direction but not trapped along z: the laser beam will tend to pull small particles in toward the central optical axis, propel them toward the focus, and keep pushing them out the other side of the trap. By employing a large numerical aperture, our apparatus provides excellent trapping in all three directions xyz.

We will investigate the motions of the particle in the xy directions only. Consequently, in the discussion that follows, when forces, impulses, velocities or other vector quantities are written without vector notation (F instead of $\mathbf{F}$), they represent the x-component of the corresponding vector quantity.

The ray optics in Figure 1 illustrate how laser beam refraction generates a trapping force. The laser beam is directed in the positive z direction and brought to a focus by a microscope objective. Note that, owing to wave diffraction, the focal region has nonzero

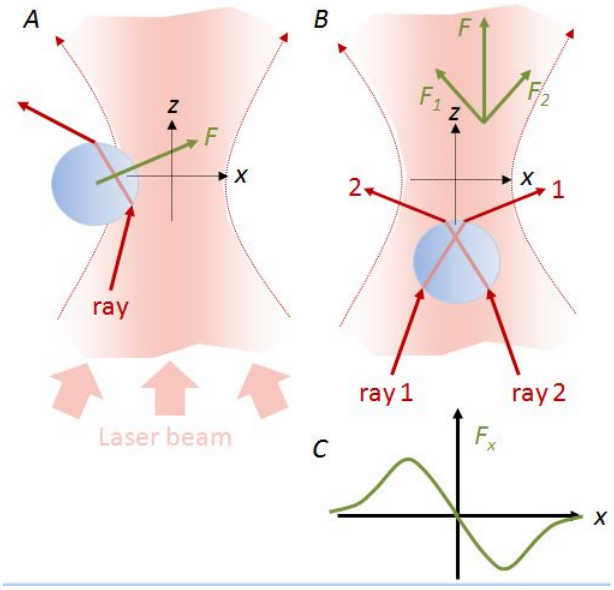

Figure 1: Ray optical model for the trapping force at the focus of a laser beam. A particle displaced horizontally *(A)* or vertically *(B)* from the focus (at $x = y = z = 0$) refracts the light away from the focus, leading to a reaction force that pulls the particle toward the focus; *(C)* Schematic of the restoring force F_x *versus* displacement x of the particle from the trap center. Near the beam focus $x = 0$, $F_x \approx -kx$.

width in the xy direction. Near the beam focus a spherical dielectric particle alters the direction of a ray by refracting it as shown in 1A. Momentum conservation implies that the particle experiences a force, indicated by $\mathbf{F}$ in the figure, that is directed toward the beam focus. If the particle is located below the focus, it refracts the converging rays (such as rays 1 and 2) as shown in 1B. The corresponding reaction forces $\mathbf{F}_1$ and $\mathbf{F}_2$ acting on the particle give a vector sum $\mathbf{F}$ that is again directed toward the laser focus. The refractive scattering at any location in the vicinity of the focus results in what is called the gradient force—-a force that pulls the particle into the beam focus.

Specular reflection of photons at the boundaries between the sphere and the medium result in a force that is also position dependent but largely directed upward in the direction of the laser photons. This is called the scattering force. At any point, the scattering force is proportiona to the laser intensity and in the direction of the photon flow and the gradient force is proportional to and in the direction of the gradient of the laser intensity. If the gradient force is larger than the scattering force, the net laser force can be described as a restoring force about an equilibrium position, which is slightly downstream of (above) the actual focal spot of the laser.

What other forces act on the particle? The laser in our apparatus is directed vertically upward—along the same axis as gravitational and buoyancy forces. For silica spheres, which are more dense than water, the net result is a downward force. Bacteria are less dense than silica but still more dense than water; therefore they are also subject to a weak net downward force. As in the case of a standard mechanical spring subject to a gravitational force, the consequence of these constant forces in the $\pm z$-direction is that the particle's equilibrium position in the trap, which defines $\mathbf{r} = 0$, moves slightly down along the z-axis. The term "trapping force" will refer to the laser force as well as the gravitational and buoyancy forces.

The fluid environment supplies two additional important forces to the particle. The particles that we study with our laser tweezers are suspended in water. The water molecules have velocities that are governed by the Maxwell-Boltzmann distribution: The direction of each molecule's motion is random and so the average molecular velocity $\mathbf{v}$ is zero, but the average molecular speed v is *not* zero. The mean squared velocity is therefore

nonzero, and it is related to the temperature T (Kelvin) by the equipartition theorem:

$$\frac{1}{2}m\left\langle v^2\right\rangle = \frac{3}{2}k_BT \tag{1}$$

Here v is the molecular speed (in three dimensions) and $k_B = 1.38 \times 10^{-23}$ J/K is Boltzmann's constant.

Exercise 1 *Use Eq. 1 to estimate the root-mean-square (rms) velocity of water molecules near room temperature (23 C). Give your answer in m/s.*

Therefore, even if there is no bulk movement of the water, a small particle immersed in water is continuously subjected to collisions from moving water molecules. For a one-micron particle in water at room temperature, these collisions occur at a rate $\sim 10^{19}$ per second. If the particle moves relative to the fluid at a speed v, the impulses from these collisions add up to give a net drag or viscous force that opposes the relative motion:

$$F_{\text{drag}} = -\gamma v \tag{2}$$

where γ is the drag coefficient. For a sphere of radius a, γ is given by the Einstein-Stokes formula

$$\gamma = 6\pi\eta a \tag{3}$$

where η is the dynamic viscosity of the fluid.

If the particle is stationary with respect to the fluid ($v = 0$) the impulses from the random collisions of water molecules add up to zero net force, but only in a time-averaged sense. At each instant of time the collisions coming from different directions do not balance out precisely; hence the particle is subject to a very weak and rapidly fluctuating random force. If no other forces act on the particle, this weak fluctuating force, denoted $F(t)$, tends to push the particle slowly through the fluid along a random, irregular trajectory. This random motion is known as *Brownian motion* and is readily observed under a microscope when any small (micron-sized or smaller) particle is suspended in a fluid. When the particle is trapped at the focus of an optical tweezers, the Brownian force acts as a continuous perturbation that pushes the particle in random directions.

Exercise 2 *You can estimate the average speed of Brownian motion from the fact that the speed of the microscopic particle at temperature T must also satisfy the equipartition theorem (1). For a silica sphere of diameter $1\,\mu m$ and a density of 2.65 g/cm^3, what is its rms velocity along any axis at room temperature? Is your result still valid if the particle is in an optical trap?*

The local environment may produce other forces on a small particle. The silica particles in our experiment can adhere to a glass coverslip. A vacuole in a plant cell may be pulled through the cell by a molecular motor, while a swimming bacterium generates its own propulsion force by spinning its flagella. These additional forces compete with the trapping and fluid forces. This means that they can be used to measure the strength of the trap and vice versa: Subsequent sections describe how to use the physics of Brownian motion and viscous drag to determine the strength of the trapping and drag forces.

We will need to know the position x of the particle with respect to the trap. In principle we could calculate x by analyzing microscopy images collected with a camera. In practice this does not work well because the displacements are very small and fluctuate rapidly. We can obtain higher precision and faster time resolution if we detect the particle's displacement indirectly by measuring the laser light

that the particle deflects from the beam focus. Light scattered by the particle travels downstream (along the laser beam axis) and—in our apparatus—is measured on a quadrant photodiode detector (QPD). The QPD is discussed in the experimental section. Here we merely note that as the particle moves from the trap into either the $+x$ or $-x$-direction, it deflects some of the laser light in the same direction, and the QPD reports this deflection by generating a positive or negative voltage V.

For small displacements x of the particle from the beam focus, the QPD voltage is linear in the displacement ($V \propto x$). Consequently, we can write

$$x = \beta V \tag{4}$$

We will refer to β (units of meters/volt) as the *detector constant*. Because the voltage generated by the QPD depends on the total amount of scattered light, β depends on the laser power as well as the shape and size of the particle and other optical properties of the particle and liquid.

Analysis of Trapped Motion

How can we measure the strength of the trap? Suppose that a particle, suspended in water, is held in the optical trap. If we move the microscope stage (that holds the sample slide) in the x direction, the trap (whose position is determined by the beam optics) will remain fixed; therefore by moving the stage at a velocity $\dot{x}_{\text{drive}}$ we will move the water at the same velocity, so that the fluid and the trapped particle are in relative motion. Now, the particle will experience three forces as follows:

1. *The trapping force* - Near the trap center, the trapping force can be modeled as a Hooke's Law restoring force $-kx$, where k is the trap stiffness (newtons/meter) and x is the particle's displacement from the trap origin.

2. *The viscous drag force* - The velocity of the particle relative to the fluid is $\dot{x} - \dot{x}_{\text{drive}}$, so the particle experiences a drag force $-\gamma(\dot{x} - \dot{x}_{\text{drive}})$, where γ is a drag coefficient with units of newton-sec/meter.

3. *The Brownian motion force* - The rapidly fluctuating force $F(t)$ averages to zero over time, $\langle F(t) \rangle = 0$, but has a non-zero mean-squared value $\langle F(t)^2 \rangle > 0$.

While the Stokes Einstein prediction (Eq. 3) for γ is accurate for a spherical particle in an idealized fluid flow environment, the real γ is influenced by proximity to surfaces (the microscope slide) and is sensitive to temperature and fluid composition through the viscosity η. Thus it is appropriate to determine γ experimentally and compare it with the Stokes Einstein prediction. A complete calibration includes a determination of the trap stiffness k, the detector constant β, and the drag coefficient γ.

We use the calibration method designed by Tolic-Norrelykke, et al. (See also Berg-Sorensen and Flyvberg.) The basic idea is to drive the stage back and forth sinusoidally with a known amplitude and at a constant frequency f_d and measure (via the QPD detector voltage V) the particle's response to the fluid and trapping forces. Essentially we oscillate the fluid while the particle resides in the trap and we observe the response to the oscillations and to the Brownian force. Because the physics of heavily damped motion of a particle in a fluid are well understood, the frequency characteristics of $V(t)$ will reveal the parameters k, β, γ with good precision.

We hold the particle in the optical trap while the microscope stage (i.e., the fluid) is

driven back and forth such that x_{drive} oscillates at frequency f_d. The location of the stage (with respect to the trap) oscillates as

$$x_{\rm drive}(t) = A\cos(2\pi f_d t) \tag{5}$$

and the fluid has a velocity

$$\dot{x}_{\rm drive}(t) = -A2\pi f_d \sin(2\pi f_d t). \tag{6}$$

Newton's 2nd law then takes the form

$$m\ddot{x}(t) = F(t) - kx - \gamma(\dot{x} - \dot{x}_{\rm drive}) \tag{7}$$

where m is the particle mass and x is its displacement with respect to the trap.

We are familiar with underdamped oscillators, for which the drag term $-\gamma\dot{x}$ in Newton's law is small in comparison to the acceleration ("inertial") term $m\ddot{x}$. For such oscillators the acceleration is largely determined by the other (nonviscous) forces acting on the particle. However, the drag coefficient γ in a fluid generally scales as the radius a of the particle, whereas the mass m scales with the particle's volume, $m \propto a^3$. Consequently, for sufficiently small ($a \sim \mu$m) particles in water, the inertial term is far smaller than the drag term, $|m\ddot{x}| \ll |\gamma\dot{x}|$. Under such conditions the oscillator is overdamped, and (to an excellent approximation) we may drop the inertial term from Eq. 7. The particle velocity is then determined by the balance between the viscous force and the other forces acting on the particle. Physically this means that, if any force is applied to the particle, the particle "instantly" (see *Exercise* below) accelerates to its terminal velocity in the direction of the applied force. When we drop the $m\ddot{x}$ term the equation of motion becomes quite a bit easier to work with:

$$F(t) = kx + \gamma(\dot{x} - \dot{x}_{\rm drive}) \tag{8}$$

where $F(t)$ is the randomly fluctuating Brownian force.

Exercise 3 *Suppose that the drag force $-\gamma\dot{x}$ is the only force acting on the particle so that the equation of motion becomes $m\ddot{x} = -\gamma\dot{x}$. Solve this equation for $\dot{x}(t)$ for a particle with an initial velocity v_0. Show that the velocity decays exponentially to zero and give an expression for the time constant involved. (This would also be the time constant for reaching terminal velocity when there are additional forces acting on the particle.) What is the time constant for a silica sphere of radius $a = 1$ μm moving through water ($\eta \simeq 10^{-3}$ N-s/m^2)? Integrate your solution for $\dot{x}(t)$ (assuming $x_0 = 0$) to determine $x(t)$. If the sphere has an initial velocity $v_0 = 1$ cm/s, approximately how far does it travel before coming to rest? Give your answer in microns (μm).*

Dropping the $m\ddot{x}(t)$ term in Eq. 7 is equivalent to assuming that the time constant for reaching terminal velocity is negligible. To solve the resulting Eq. 8, first collect the x and $\dot{x}$ terms on the right side and multiply throughout by $e^{kt/\gamma}$

$$\begin{aligned}(F(t) + \gamma\dot{x}_{\rm drive})\, e^{kt/\gamma} = \\ \gamma\left((k/\gamma)\, x e^{kt/\gamma} + \dot{x}e^{kt/\gamma}\right)\end{aligned} \tag{9}$$

Recognizing the right hand side as a derivative, we find

$$x(t) = x_T(t) + x_{\rm response}(t) \tag{10}$$

where

$$x_T(t) = \frac{1}{\gamma}\int_{-\infty}^{t} F(t')e^{2\pi f_c(t'-t)}\, dt' \tag{11}$$

$$x_{\rm response}(t) = \int_{-\infty}^{t} \dot{x}_{\rm drive}\,(t')\, e^{2\pi f_c(t'-t)}\, dt' \tag{12}$$

and

$$f_c = \frac{k}{2\pi\gamma} \tag{13}$$

has units of frequency (1/time).

Exercise 4 *Derive Eqs. 10-12 above. Also evaluate the integral for* $x_{\text{response}}(t)$ *(Eq. 12) given the driving velocity of Eq. 6. Show that* $x_{\text{response}}(t)$ *is sinusoidal oscillations with an amplitude given by Eq. 25.*

Equation 10 shows that the motion $x(t)$ has two components. $x_{\text{response}}(t)$ is an oscillatory response to the periodic motion of the fluid, while $x_T(t)$ is a fluctuating term that is determined by the recent values of the Brownian force $F(t)$. Since $x_T(t)$ contributes a sizeable, random component to the motion, $x(t)$ is noisy and non-periodic: There is little to be gained by tracking the specific values it takes during a particular interval of time. We can learn a lot more from a statistical approach in which we study the frequency components of $x(t)$. For that we need to return to Eq. 8 and investigate the Fourier transform of the motion.

Consider the Fourier transforms of a trajectory $x(t)$

$$\tilde{x}(f) = \int_{-\infty}^{\infty} x(t)\, e^{-2\pi i f t}\, dt \tag{14}$$

and the Brownian force $F(t)$

$$\tilde{F}(f) = \int_{-\infty}^{\infty} F(t)\, e^{-2\pi i f t}\, dt. \tag{15}$$

Here the complete Fourier transform is evaluated for frequencies f covering both halves of the real axis $-\infty < f < \infty$ so that the inverse Fourier transform properly returns the original function. For example, $x(t)$ is recovered from the inverse Fourier transform of $\tilde{x}(f)$:

$$x(t) = \int_{-\infty}^{\infty} \tilde{x}(f)\, e^{2\pi i f t}\, df \tag{16}$$

Note that $\tilde{x}$ has units of m/Hz and $\tilde{F}$ has units of N/Hz.

A relationship between $\tilde{x}$ and $\tilde{F}$ is readily obtained by taking the Fourier transform of the equation of motion, Eq. 8. That is, multiply both sides by $\exp(-2\pi i f t)$ and integrate over dt. The result is

$$\begin{aligned}\tilde{F} &= k\tilde{x} + \gamma 2\pi i f \tilde{x} \\ &\quad + \frac{2\pi\gamma f_d A}{2i}\left(\delta(f+f_d) - \delta(f-f_d)\right)\end{aligned} \tag{17}$$

To get Eq. 17, the Fourier transform of $\dot{x}(t)$ has been replaced by $2\pi i f$ times the Fourier transform of $x(t)$—as can be demonstrated by evaluating $\dot{x}$ starting from Eq. 16. The explicit form of $\dot{x}_{\text{drive}}$ as given by Eq. 6 has been used and the Fourier transform of $\sin(2\pi f_d t)$, which is given by $(\delta(f-f_d) - \delta(f+f_d))/2i$ has been applied. Solving for $\tilde{x}$ then gives

$$\begin{aligned}\tilde{x} &= \frac{\tilde{F}}{2\pi\gamma\,(f_c + if)} \\ &\quad - \frac{f_d A}{2i\,(f_c + if)}\left(\delta(f+f_d) - \delta(f-f_d)\right)\end{aligned} \tag{18}$$

where we have replaced k by $2\pi\gamma f_c$ (Eq. 13).

Equation 18 is a perfectly good description of the particle response x—it just happens to be Fourier transformed. We will use it to extract information from measurements of $x(t)$.

Discrete Fourier transforms

Although we have treated time t as a continuous variable that spans the range $-\infty \to +\infty$, in actual experiments we collect a finite number of data values over a finite time interval τ. A typical data set is a discrete sampling of the QPD voltage $V(t) = \beta x(t)$ over a time interval $\tau \simeq 1-2$ sec, with measurements acquired at a uniform digitizing rate $\sim$ 100,000 samples per second. For this discussion, we can consider β as given, so that the data consists of values of $x(t_m)$ at a set of sampling times t_m.

Let's assume that measurements of $x(t)$ are made during the time interval from $-\tau/2 < t < \tau/2$. The integration in Eq. 14 needs to

be truncated so that t falls within this interval only. Of course, we expect that we will recover the previous results in the limit as $\tau \to \infty$.

To analyze finite, discrete data sets, we need to define the *discrete Fourier transform* (DFT). The DFT of $x(t)$ is the version of the Fourier transform that is comparable to Eq. 14 but applies to a large (but finite) number L of discretely sampled $x(t_m)$ values. The finite integration is performed according to Simpson's rule (without end corrections). If the measurement times t_m are spaced $\Delta t = \tau/L$ apart in time and the integration is over the range $-\tau/2 \le t \le \tau/2$, then we can write $t_m = m\Delta t$ with $-L/2 \le m \le L/2$. Then the DFT becomes

$$\tilde{x}(f_j) = \sum_{m=-L/2}^{L/2} x(t_m) e^{-2\pi i f_j m \Delta t} \Delta t \qquad (19)$$

For our data sets, this DFT is expected to accurately reproduce the true Fourier transform for both positive and negative frequencies up to one half the digitizing rate. While it is defined for any f_j, the DFT is normally evaluated at fixed frequencies $f_j = j\Delta f$ where

$$\Delta f = \frac{1}{\tau} \qquad (20)$$

and $-L/2 \le j \le L/2$. That is, both $x(t)$ and its DFT $\tilde{x}(f_j)$ contain the same number of points, but each of the $\tilde{x}(f_j)$ has both a real and an imaginary part. However, the two parts are not independent. If all the $x(t)$ are real, it is easy to demonstrate that $\tilde{x}(-f) = \tilde{x}^*(f)$. That is, for opposite frequencies, f and $-f$, the real parts are equal and the imaginary parts are negatives of one another. Thus $x(t_m)$ and $\tilde{x}(f_j)$ both contain the same number of independent quantities. The two sets are just different ways of representing the same data.

The power spectrum

Another issue arises because the theory of Brownian motion does not specify $\tilde{F}$. At any frequency, $\tilde{F}(f)$ is a complex number z with the general forms, $z = x + iy = re^{i\theta}$, where x and y are the real and imaginary parts of z, r is the modulus and $\theta = \arctan(y/x)$ is the argument or phase of z. The theory only predicts the *intensity* given by the modulus squared: $r^2 = x^2 + y^2 = zz^*$, where $z^* = x - iy$ is the complex conjugate of z. It does not predict the real or imaginary parts of z or the phase. Moreover, the theory predicts that the Fourier intensities $\tilde{F}\tilde{F}^*$ obtained from a finite Fourier transform will be proportional to the integration interval τ. The theory thus gives a result that is independent of τ only if the intensities are divided by τ. The traditional characterization of the strength of the fluctuating force $F(t)$ is therefore its *power spectrum* or *power spectral density* (PSD), defined as

$$P_F(f) = \frac{\tilde{F}(f)\tilde{F}^*(f)}{2\tau} \qquad (21)$$

With the factor of two in the denominator the PSD gives the rms values for the underlying oscillator intensities.

The Brownian force is actually expected to have equal power at all frequencies—that is, $P_F(f)$ is independent of f. Furthermore, in order that the average speed of the particle obeys the equipartition theorem (Eq. 1), the strength of the Brownian force must depend directly on both temperature T and the viscous drag coefficient γ:

$$P_F(f) = 2\gamma k_B T \qquad (22)$$

where k_B is Boltzmann's constant. Equation 22 is an example of a *fluctuation-dissipation theorem* relating energy loss mechanisms (the damping coefficient γ) with fluctuating thermal forces (the Brownian PSD P_F).

After all, it is the combination of the Brownian force and the viscous drag that must keep the particle moving with the average speed indicated by Eq. 1.

For any frequency component f of a given trajectory $x(t)$, $\tilde{x}(f)$ is also a random variable with a mean of zero. The square of its Fourier transform, $\tilde{x}\tilde{x}^*$, will have a non-zero mean and we should anticipate that (like $\tilde{F}\tilde{F}^*$) this is also proportional to integration time τ. The power spectral density for $\tilde{x}$

$$P(f) = \frac{\tilde{x}(f)\tilde{x}^*(f)}{2\tau} \tag{23}$$

is then also independent of τ.

Because $\tilde{x}(-f_j) = \tilde{x}^*(f_j)$, it should be apparent from Eq. 23 that $P(-f_j) = P(f_j)$. For this reason we only analyze the power spectrum for $f > 0$.

To see the relationship between the power spectrum for x and F, consider the case where the stage oscillations are turned off, $A = 0$, so that the delta functions do not contribute to $\tilde{x}(f)$. Then multiply each side of Eq. 18 by its complex conjugate and divide by 2τ to get

$$\begin{aligned} P(f) &= \frac{P_F(f)}{2\pi^2\gamma^2(f_c^2 + f^2)} \\ &= \frac{k_B T}{\pi^2\gamma(f_c^2 + f^2)} \end{aligned} \tag{24}$$

Notice that $P_F(f)$ has units of N^2/Hz and $P(f)$ has units of m^2/Hz. It actually makes sense to consider these functions as a density. For example, if we integrate $P(f)$ over a sufficiently small interval Δf centered around a frequency f_0, we obtain $P(f_0)\Delta f$. This value represents the mean squared amplitude of the oscillatory component of $x(t)$ at frequency f_0.

If the stage oscillations are turned back on, how do they affect the power spectrum? We can refer to Eq. 18 and see how the two delta function terms (resulting from the stage motion of amplitude A at the drive frequency f_d) contribute. The inverse Fourier transform of the delta function term shows that this represents oscillation at the drive frequency f_d with an amplitude A'

$$A' = \frac{A}{\sqrt{1 + f_c^2/f_d^2}} \tag{25}$$

The case $f_c \ll f_d$ corresponds to a weak trap (small k) or a high drive frequency f_d. In this case $A' = A$ and the amplitude of the particle oscillation equals the amplitude of the stage oscillation. For stronger traps or lower drive frequencies, A' is smaller than A by the factor of $\sqrt{1 + f_c^2/f_d^2}$; the particle oscillates with smaller amplitude than the stage. Equation 25 shows how the trap attenuates the oscillation of the particle, relative to that of the stage.

Therefore the power spectrum of the particle in the trap is the sum of two terms.

$$\begin{aligned} P(f) &= \frac{k_B T}{\pi^2\gamma\left(f_c^2 + f^2\right)} \\ &\quad + \frac{A^2}{2\left(1 + f_c^2/f_d^2\right)}\delta\left(f - f_d\right) \end{aligned} \tag{26}$$

$$= P_T(f) + P_{\text{response}}(f) \tag{27}$$

The first term $P_T(f)$ describes the thermal (Brownian) motion of the particle, in the absence of any oscillation of the stage. The second term $P_{\text{response}}(f)$ contains the delta function and is the consequence of the stage oscillations. The coefficient of the delta function provides that, when we integrate $P_{\text{response}}(f)df$ over a narrow frequency interval that contains f_d, we will obtain the squared amplitude $A'^2/2$, *i.e.*, the mean squared amplitude of the particle's oscillation at f_d.

Keep in mind that these predictions for the power spectrum come from Eq. 18, which was derived from continuous Fourier transforms, assuming an infinite measurement time, whereas our data are collected in a discrete

sampling over a finite interval τ. Therefore we do not expect our data to reproduce these predicted spectra perfectly. For example, you may imagine that calculating $P(f)$ from a data set that consists of only (say) 10 samplings of x during a time interval of only $\tau = 1$ msec would give a poor representation of the true spectral behavior of x.

However our results will improve if we work in the limit $\tau \to \infty$. It is not practical to achieve this limit by taking ever longer measurements, with correspondingly larger data sets. Data sets larger than a few hundred thousand data points are tedious to manage and analyze; the improvement in the result does not justify the extra effort of handling and processing such large data arrays. A far better way to approach the limit of $\tau \to \infty$ experimentally is just to collect a number of data sets of duration $\tau \sim 1$ sec and then average the $P(f)$ results obtained.

The two terms in Equation 26 (see Tolic-Norrelykke (2006)) have fairly simple behavior. $P_T(f)$ is nearly constant for $f \ll f_c$ and then falls off as $\sim 1/f^2$ for $f \gg f_c$. f_c plays the role of a "cutoff frequency." Fluctuations in the position of the particle at frequencies higher than f_c are suppressed by the viscous drag. The second term $P_{\text{response}}(t)$ includes a δ-function at the drive frequency f_d. The particle is predicted to oscillate in the trap at the same frequency at which the fluid moves back and forth.

Equation 26 is for the particle's position x, while we will actually measure the QPD voltage $V(t_i) = x(t_i)/\beta$. Our experimentally determined power spectrum density will be the average of power spectrum density for the voltage $\tilde{V}\tilde{V}^*/2\tau$, not $\tilde{x}\tilde{x}^*/2\tau$. As the Fourier transform is linear, the Fourier transform of $V(t)$ is related to that of $x(t)$ by the calibration factor β:

$$\tilde{V} = \tilde{x}/\beta \tag{28}$$

Accordingly, if we experimentally measure $V(t)$ and then calculate $P_V(f)$, the PSD of the voltage data, then we expect

$$P_V(f) = P(f)/\beta^2. \tag{29}$$

After each τ-sized $V(t)$ is measured, its discrete Fourier transform $\tilde{V}(f_j)$ is calculated and then used to determine its power spectrum density $P_V(f_j) = \tilde{V}(f_j)\tilde{V}^*(f_j)/2\tau$. After sufficient averaging of such $P_V(f_j)$, the predicted behavior will begin to appear—a continuous part from P_T and a sharp peak at f_d due to P_{response}. This PSD is fit to the prediction of Eq. 26 (with Eq. 29) to determine the parameters of the optical trap: the trap constant β, the drag coefficient γ and the force constant $k = 2\pi\gamma f_c$.

Exercise 5 *In the optical trapping literature, typical reported values for the cutoff frequency are in the range $f_c \simeq 10^2 - 10^3$ Hz. Assuming that these correspond to spherical particles of radius $a = 0.5\,\mu m$ in water at room temperature (295 K), estimate the magnitude of the trap stiffness constant k. Give your answer in $pN/\mu m$.*

Exercise 6 *Make two sketches of the $P_T(f)$ term in Eq. 26 for a particle in a trap with $f_c = 100$ Hz. The first sketch should use linear scales (P vs. f), while the second should use a log-log scale ($\log P$ vs. $\log f$) for $10^{-2} f_c \leq f \leq 10^2 f_c$.*

Comparing the predicted $P_V(f)$ with one actually determined from the measured QPD voltage vs. time data is done in two steps: one for the thermal component $P_T(f)$ and one for $P_{\text{response}}(f)$ containing the delta function response to the stage oscillations. We will begin with a discussion of the latter.

The main theoretical feature of a delta function is that its integral over any region containing the delta function is one. Thus, the

predicted integral W of the $P_V(f)$ of Eq. 29 associated with the delta function in Eq. 26 is easily seen to be

$$W = \frac{1}{\beta^2}\int_0^\infty P_{\text{response}}\, df = \frac{A^2}{2\beta^2\left(1+(f_c/f_d)^2\right)} \quad (30)$$

In the experiment, the drive frequency f_d will be chosen so that there will be an exact integer number of complete drive oscillations over the measurement interval τ. This makes f_d one of the frequencies at which the $P_V(f_j)$ is evaluated and should produce one high point in this PSD. You will determine the height of that point above the thermal background and multiply by the spacing Δf between points to get the experimental equivalent of integrating $P_V(f)$ over the delta function. In rare cases, you may see the experimental delta function spread over several f_j centered around f_d. In these cases, the experimental integral is the sum of the amount these points exceed the thermal background times Δf.

The experimental value of W obtained this way is then used with Eq. 30 and the known stage oscillation amplitude A, the frequency f_d, and the value of f_c determined in the next step to determine the trap constant β.

The force constant k and the drag coefficient γ are found by fitting the non-δ-function portion of the experimental $P_V(f)$ ($f \neq f_d$) to the prediction of Eq. 26 (with Eq. 29). That is, for all values of f except $f = f_d$, the predicted PSD can be written

$$P_V(f) = \frac{k_B T}{\pi^2\beta^2\gamma\left(f_c^2+f^2\right)} \quad (31)$$

For fitting purposes, this equation is more appropriately expressed

$$P_V(f) = \frac{B}{1+f^2/f_c^2} \quad (32)$$

where B is predicted to be

$$B = \frac{k_B T}{\pi^2\beta^2\gamma f_c^2} \quad (33)$$

The experimental $P_V(f_j)$ is then fit to Eq. 32 over a range of f (not including the point at $f = f_d$) which then determines the fitting parameters B and f_c.

With f_c determined directly from this fit, the experimental W is used with Eq. 30 to determine β. Then, assuming T is equal to the measured room temperature, the fitted B is used in Eq. 33 with f_c and β to determine the value of γ. Finally, the force constant $k = 2\pi\gamma f_c$ (Eq. 13) is determined and the three trap parameters γ, β and k are then known.

Apparatus

Our optical trap is based on the design of Appleyard *et al.*[3] It uses an inverted microscope to focus an infrared diode laser beam onto the sample, and it detects the deflection of that beam with a quadrant photodiode detector (QPD). The system also illuminates the sample with white light and and generates an image of the sample on a video camera. The details are somewhat complex, as the same optical elements perform several functions simultaneously. The layout is described below. We refer to the xy plane as the plane of the sample stage, while the $+z$-direction is the direction of propagation of the laser beam as it passes through the xy plane.

Refer to the figure 2 and locate the major elements of the system:

1. *The optical path for the infrared laser:* A semiconductor diode laser generates an intense infared beam (λ = 975 nm) that is collimated and aimed into the back aperture of the lower microscope

[3] See References.

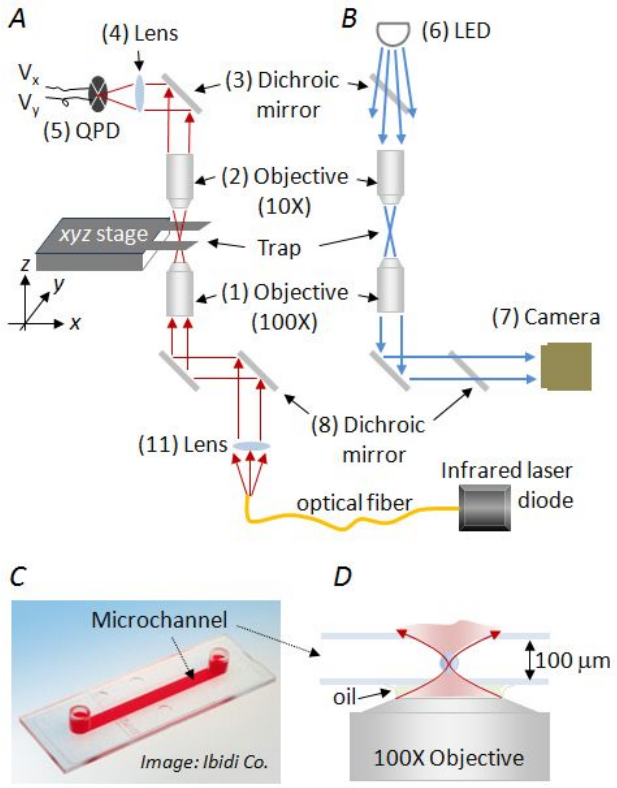

Figure 2: *A* and *B* show two views of the optical system, illustrating the paths of the infrared trapping rays (red arrows in *A*) and the visible illumination rays (blue arrows in *B*) as they pass through the same optical elements. The sample is contained in a 100 μm-deep microchannel slide *C*, at the focus *D* of the 100× oil-immersion lens.

objective (#1) (100× Nikon 1.25 NA, oil-immersion); the objective brings the beam to a focus at the sample, forming the optical trap. The upper microscope objective (#2) captures and recollimates the infrared light that has passed through the sample and directs this energy upward. A dichroic (infrared-reflecting) mirror (#3) then deflects the beam toward a converging lens (#4), which focuses the beam to form a spot on a quadrant photodiode detector (#5, QPD). The voltages V_x and V_y from the QPD are used to determine the position of the particle in the xy plane.

2. *The optical path for visible light:* An LED (#6) generates white light that passes through the dichroic mirror (#3) and is focused by the upper objective (#2) onto the sample. Transmitted white light is gathered by the lower objective (#1) and brought to an image at the CCD camera (#7). The CCD captures a video image of the sample, although the IR laser beam is not visible in the image. The dichroic mirror (#8) in the optical path near the CCD camera transmits the white light of the LED, while it reflects IR laser light.

3. *The microscope stage:* The sample is contained in a small flow cell or slide consisting of two parallel glass coverslip windows separated by approximately 100μm. The slide is held between the upper and lower objectives by a moveable *xyz* ("3-axis") stage. The sample position in the xy-plane can be manually adjusted by turning the two micrometers labelled X and Y on the stage. The stage also has piezoelectric actuators and driver circuitry that allows the computer to take control of xy motion of the stage. The focus of the CCD camera image is adjusted by turning the z-direction fine-control micrometer on the stage, thus raising or lowering the slide. Keep in mind that if you raise or lower the slide too far, it will crash against the microscope objective. Please take care to avoid such contact as the objectives are quite expensive.

4. *The IR laser:* The diode laser is a semiconductor device that outputs its beam to a single-mode optical fiber. A converging lens (#11) receives the light exiting

the fiber and collimates it to a beam with a diameter of $\sim$ 10 mm, or sufficient to fill the back aperture of the trapping objective (#1). A set of mirrors and the dichroic mirror (#8, infrared-reflecting) are used to steer the laser beam along the central axis of the objective.

In this design the infrared laser serves two roles. It traps the particle at the focus, and it is also used to detect the motion of the particle within the trap. If there is no particle in the trap, the infrared laser beam propagates along the optical axis of the instrument, i.e., along the common cylindrical axis of the microscope objectives). The recollimated beam exiting the upper objective travels parallel to the optical axis, and the converging lens (#4) brings this beam to a focus just a bit in front of the center of the QPD. However if a small particle is near the laser focus, the beam is refracted away from the optical axis. The collimated beam leaving the upper objective will then propagate at an angle to the optical axis, and so it is focused by the converging lens (#4) to a spot that is displaced from the center of the QPD. The QPD reports this displacement as a voltage V, which is proportional to the particle's displacement x from the laser focus (see Eq. 28). Actually, the QPD detects deflections in the both the x and y directions, reporting two independent voltages V_x and V_y that you will measure.

Laser Safety

Note that although this experiment is not dangerous, any eye exposure to the infrared laser beam would be very dangerous. The beam is very intense, with a power of several hundred mW, and it is invisible. Serious and permanent eye injury could result if the beam enters your eye. **Proper laser eye safety precautions must be used at any time that the laser is running.**

The apparatus is designed to keep the infrared laser beam enclosed within its intended optical path and away from your eyes. The instrument is safe to use as long as the laser remains enclosed. Therefore, laser safety means that you should not operate the laser when the beam enclosure is open or any portion of the optical pathway has been opened or disassembled. If you open or disassemble any components while the laser is powered you could expose yourself to the IR beam and suffer a potentially severe injury. Do not attempt to align or adjust any part of the infrared laser optical path.

The only point in the apparatus where the beam leaves its confining path is at the sample slide, between the two microscope objectives. In this region the beam is strongly converging/diverging and is not likely to present a hazard to the user. However you should use common sense and avoid diverting the beam out of this region. Do not place shiny, metallic or reflective objects like mirrors or foil into that region. Do not put your face close to the slide if the laser is on.

Experimental overview

The basic tasks are to first calibrate the apparatus as described previously to measure the trap strength, calibration constant, and drag coefficient for small particles of silica (SiO_2), roughly 0.5-1.5 μm in diameter. Having gained this experience with the apparatus, you can then experiment with biological trapping by measuring, e.g., the force generated by a swimming bacterium. Note that it takes a couple of days to prepare the bacterial culture for the experiment, so you will need to plan ahead by notifying your instructor of the date when you plan to perform the bacterial study.

The basic plan is to

1. Become familiar with instrument. Learn to use the software, camera, power supplies, etc.

2. Calibrate the camera image by acquiring an image of a stage reticle slide, which has known micron-sized scales imprinted on it. Measure these scales in pixels on the image to determine the camera image's calibration in μm/pixel.

3. Calibrate the microscope stage motion. The stage can be moved with the manual micrometers and with two modes of piezo-controlled motion (with and without strain-gauge feedback). You will need to know how the stage moves in each mode.

4. Load a sample with silica spheres of one size and adjust the apparatus settings. With no stage motion, measure the PSD and determine f_c.

5. Activate stage motion and measure the PSD. Identify the delta-function. Fit to obtain the three calibration parameters.

6. Measure as a function of laser power and determine laser power dependence of k, γ, β.

7. Repeat with different size particle.

8. Use the trap with at least one biological sample.

Hardware

Data acquisition board

The computer communicates with the tweezer apparatus through a (National Instruments PCI-MIO-16E-4) multifunction data acquisition board (DAQ) that is inside the computer. See Figure 3.

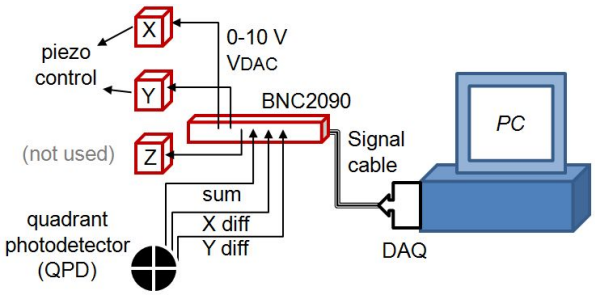

Figure 3: Schematic of electronic interface between computer and tweezer apparatus. The DAQ board in the PC has an analog-to-digital converter that reads data from the QPD, as well as digital-to-analog converters that supply control voltages for the xy positioning of the microscope stage.

The DAQ board supplies voltages that control the piezoelectric drivers, which move the microscope slide in the xy plane. It also reads voltages from the quadrant photodetector (QPD). The QPD voltages are the raw data for analysis of particle motions in the trap.

A cable from the DAQ card runs out of the PC to an interface box (National Instruments BNC-2090) that has convenient BNC jacks for connecting coaxial cables between the various apparatus components and tapping into the DAQ input and output voltages.

Two components of the DAQ board used in this apparatus are its analog to digital converter (ADC) and two digital to analog converters (DACs). The ADC can read analog voltages from -10 to 10 V at speeds up to 500,000 readings per second, and the DACs can produce output voltages in this same range that can change at similar speeds. The ADC has a high speed switch called a multiplexer that allows it to read voltages on up to

eight different inputs.

Laser

The (Thorlabs PL980P330J) laser diode is premounted to a single-mode fiber which brings it to the apparatus. It is mounted on a temperature stabilized plate kept at constant temperature by the (Thorlabs TED200C) temperature controller. The laser current is adjusted and stabilized by the (Thorlabs LDC210C) current controller. The laser current can be read off the controller. The laser turns on at a threshold current around 100 mA and then the laser power increases approximately linearly with current over threshold. An interlock requires the temperature controller to be on before the laser current controller will operate.

Controller hub

There are six Thorlabs "T-Cube" electronic modules mounted in the (Thorlabs TCH-002) T-Cube controller hub. The modules, described below, are used to electronically control the position of the microscope slide and to control and read the quadrant photodiode detector. The hub supplies power to the modules via an external power supply. It also supplies a signal path between different modules and between all six modules and the computer's USB bus via a single USB cable.

Quadrant Photodiode Detector

A quadrant photodiode detector (Thorlabs PDQ80A) is used to produce voltages that are linearly related to the position of a particle in the neighborhood of the laser focus. It has four photodiode plates arranged as in Fig. 4 around the origin of the xy-plane. The plates are separated from one another by a fraction of a millimeter and extend out about 4 mm

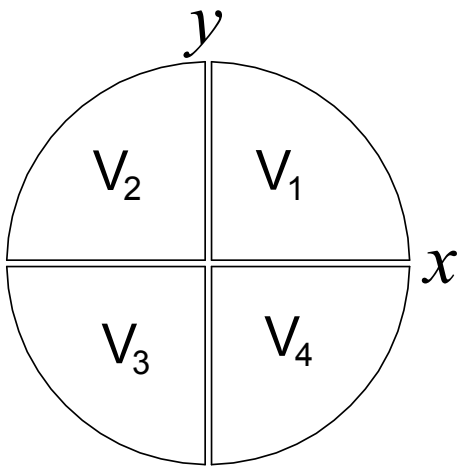

Figure 4: The QPD measures the intensity on four separate quadrant photodiodes.

from the origin. The QPD receives the infrared light from the laser and outputs a current from each quadrant proportional to the power on that quadrant.

The Thorlabs TQD-001 controller module powers the QPD and processes the currents. It does not output the currents directly. Instead, it converts them to voltages V_1-V_4 by additional electronics to produce the following three output voltages. The x-diff voltage is the difference voltage $V_x = V_1 + V_4 - (V_2 + V_3)$, the y-diff voltage is $V_y = V_1 + V_2 - (V_3 + V_4)$ and the sum voltage is the sum of all four. V_x is thus proportional to the excess power on the two quadrants where x is positive compared to the two quadrants where x is negative. Similarly for the y-diff voltage. The sum voltage is proportional to the total laser power on all four photodiodes.

With no scattering, the light that is brought to a focus by the 100× objective diverges therefrom and is refocused by the 10× objective and lens #4 so that it again comes to a focus just a bit in front of the QPD. The rays diverge from this focus before impinging

on the photodiodes so that by the time they get there, the spot is a millimeter or two in diameter and when properly centered will hit all four quadrants equally.

When a particle in the trap scatters the laser beam, the scattered light produces a complex pattern on the QPD. For small variations of the particle's position from equilibrium, V_x and V_y are proportional to the particle's x and y positions. That is $x = \beta V_x$ and $y = \beta V_y$.

While the range of linearity between the V and x is quite small—on the order of a few microns, it is still large compared to the typical motions of a particle in the trap. Significantly, this voltage responds very quickly to the particle's position so that high frequency motion (to 100 kHz or more) is accurately represented by V.

The QPD module has buttons for control of its function and it has an array of LEDs that show whether the beam intensity pattern is striking the QPD in the center (center LED lit) or off-center (off-center LEDs lit). The QPD is mounted on a manually-controlled, relatively coarse xy stage that will be centered by hand in the procedure below.

Microscope stage and piezoelectric control

The microscope stage is the component that supports the microscope slide between the 100× and 10× objectives. It provides three means for positioning the slide (and sample) in the trapping beam.

First, and very crudely, you can manually slide the stage across the table, for coarse positioning in the xy direction. You will need to do this to put your slide into the beam, but you will find it difficult to position the sample to better than about ±1 mm using this method.

Second, the stage has a set of micrometers that can be turned manually to move the stage. Over a small distance range, these micrometers function as differential screws, in which two internal threads with slightly different pitches turn simultaneously—producing a very fine ($\sim \mu$m) translating motion. As you continue turning the micrometer, the differential operation ends and the motion switches to a coarser control in which the stage moves more rapidly with each turn of the micrometer.

Third, the stage has a set of electronically-controlled piezoelectric stacks that allow the computer to move the stage along each axis. Piezoelectrics ("piezos") are crystals that expand or contract in an applied electric field, which can be generated by electrodes deposited on their crystal faces. The (Thorlabs TPZ-001) piezo controller modules supply control voltages (each up to about 75 V) to stage-mounted piezos oriented in the x, y, and z directions. Piezos provide very fine and precise control of stage motion, but only over short distance ranges: The full 75 V range of piezo voltage generates only about 20 μm of stage motion. The piezo voltage can be read from an LED indicator on the face of the module. The module also has control buttons and a knob for the various modes of controlling this voltage.

There are several ways to use the piezo controller. Manual mode, in which the voltage is controlled via the knob on the module, will be disabled and is not used in our setup. (The differential micrometers are far more convenient manual controls.) Only the following two electronically controlled methods will be used.

One method is to use the PC-DAQ to supply analog voltages in the range of 0-10 V to a Thorlabs piezo-control module. The Thorlabs module amplifies these voltages to the 0-75 V scale and sends them to the piezo. This is the fastest method and is used in our

apparatus. Alternatively, the computer can control the Thorlabs piezo-control module directly through the USB bus, bypassing the DAQ. We do not typically use this method.

Unfortunately, piezos have strong hysteresis effects. Their length, *i.e.*, how far they will move the stage, depends not only on the present electrode voltage, but also on the recent history of this voltage. One method to deal with piezo hysteresis is to obtain feedback data from a strain gauge, mounted internally inside the stage alongside the piezo. Our apparatus has one strain gauge for each of the three stage axes. They are read by the (Thorlabs TSG-001) strain gauge module, which is placed alongside the matching piezo controller in the controller hub.

The strain gauge is a position transducer with an output voltage that is very linear in the displacement caused by the corresponding piezo. This output voltage is internally wired to its corresponding piezo controller inside the controller hub. The strain, or extension of the piezo, is indicated on a scale on top of the module in units of percentage of the full scale: 0-100% for motion of about 20 μm.

Using strain gauge feedback, the controller allows you to supply USB commands requesting stage positions as a percentage (0-100) of the full scale motion (*i.e.* 0-100 % of 20 μm). In this mode, electronic feedback circuitry adjusts the actual piezo voltage to achieve that percentage. Our setup has only two strain gauge controllers, which are used only on the x and y piezos. (We are not using the z-piezo.)

Camera

A Thorlabs DCU-220C color video camera is used to observe and monitor the happenings in the trap. The camera has a rectangular CCD sensor with pixels arranged in a 1280 × 1024 cartesian grid. The pixels are square and thus distances measured on the image in pixels will scale the same way in x and y with real distances on the slide.

Software

UC480

The camera is controlled and read using the UC480 software program. This program has features for drawing or making measurements on the images, and for storing frames or video sequences. Select the Optimal colors option at load time, then hit the Open camera button—the upper left item on the upper toolbar. The default camera settings generally work fine, but if there are image problems, many camera settings can be adjusted to improve image quality. Note that there is a physical aperture directly under the camera that can be opened or closed to adjust the light. There is a bad light path in our apparatus that puts some non-image light on the camera. This artifact can be eliminated by partially closing the aperture.

Become familiar with the measurement tools and the drawing tools on the utility toolbar arrayed along the left edge of the screen. In particular, you will use the Draw circle, Draw line, and Measure tools.

Tweezers program

Most of the measurements are made from this program. It has two tabbed pages along the right. One is labeled Acquire and is for setting the data acquisition parameters, looking at the V_x and V_y signals from the QPD, and computing and averaging the PSD. The other is labeled Fit and is for fitting the PSD to the predictions of Eq. 26.

The default parameters for data acquisition should work fine. The number of points in each scan of V_x and V_y vs. t is forced to be

a power of 2 ($2^{18} = 262144$ is the default) so that fast Fourier transforms can be used. The sampling rate for the ADC is determined by dividing down the 20 MHz clock on the DAQ board. The divisor is the number of 20 MHz clock pulses between each digitization. The maximum speed of the ADC is around 250 kHz when reading two channels (V_x and V_y). The 105 default value for this divisor leads to a sampling rate around 190 kHz. With the 2^{18} samples in each scan, each scan lasts $2^{18} * 105/(20 \times 10^6\,\mathrm{Hz}) = 1.38$ s. The inverse of this time (default about 0.73 Hz) is the frequency spacing between points in the PSD.

The ADC has an instrument amplifier that allows bipolar full scale voltages from ±50 mV up to ±10 v. The F.S. range control should be set as small as possible without letting the V_x or V_y signals hit the range limits.

The two DACs used to drive the piezo controllers for the stage motion send sinusoidal waveforms with adjustable amplitudes for each DAC and with an adjustable phase between them. You can set the amplitude A_x or A_y to zero to check if stage motion in one or the other direction is picked up only in one QPD direction V_x or V_y. It is recommended that the amplitudes be set equal with a 90° phase difference so that the stage will move with nearly circular motion. This way no matter what direction the QPD's x and y responses are aligned to, the stage motion will be sinusoidal with the chosen amplitude in that direction.

Recall that the drive frequency should be made equal to one of the points in the QPD spectrum. To make this happen, set the integer M control. If the default divisor (for the ADC) of $3 \cdot 5 \cdot 7 = 105$ is used, allowed values for M would be any that can be made with single factors of 3, 5, and 7 and any number of factors of two. Another good ADC divisor is $5 \cdot 5 \cdot 4 = 100$. This gives a sampling rate of 200 kHz and allowed values of M will be any that can be made with one or two factors of 5 and any number of factors of two. Selecting disallowed values for M will disable the continue button.

Once the data acquisition parameters have been accepted—by hitting an enabled continue button—they cannot be changed without restarting the program—with one exception. The amplitude and phase of the drive waveforms can be adjusted by setting the new values in the controls for them and hitting the change amplitude button.

The fitting routine, accessed from the fit tab, has several features designed for the data from this apparatus. First note the channel selector just above the graph. It is used to switch between the two channels (A or B, i.e., the QPD x- or y-directions). The two cursors on the graph must be set to determine the points in between that will be used in the fit to Eq. 32. The PSD is normally displayed on a log-log scale, but this can be changed using the tools in the scale legend at the lower left of the graph. Our PSDs show that many high frequency and some low frequency components are being picked up in the V_x and V_y inputs. They might originate from external light sources, electrical interference, table and apparatus vibrations, etc. These unwanted signals typically appear as spikes on top of the normal Lorentzian shape of the PSD.

Spikes at the high frequency end of the PSD can be eliminated from consideration by setting the second cursor below them. In fact, fits that include too many high frequency data points tend to take too long. Be sure to include enough points above f_c, but set the high cursor so there are less than 10,000 points. Spikes between the cursors can be eliminated from the fit by setting their weighting factors to zero. This is done programmatically by

telling the program how to distinguish these spikes from the normal Lorentzian data. The criteria for eliminating the spikes thus requires an understanding of the normal and expected noise in the PSD.

Ordinary random variations in $V_x(t)$ and $V_y(t)$ over any finit time interval, lead to noise in the Lorentzian PSD that becomes smaller as more data is averaged. Look at $P_V(f)$ after averaging 20-100 scans and note that the size of the noise (not the unwanted spikes) on the vertical log scale is nearly constant. While the band of noise may appear a bit wider at higher frequencies, this is at least partially an artifact of the log f scale for the horizontal axis. At higher frequencies the points are more closely spaced so that the number of 2-sigma and 3-sigma variations appear more frequently per unit length along the f-axis. The band of noise appears more uniformly sized when looked at using a linear f-axis scaling. Uniformly sized noise on a log scale implies the fractional uncertainty in $P_V(f)$ is constant. Estimate the $\pm$1-sigma fractional uncertainty that would include about 68% of the data points in any small region of frequency. Check that this fraction is roughly constant even as $P_V(f)$ varies by one or more orders of magnitude. Enter this fraction in the control for fractional unc. Then enter the rejection criterion in the reject control. For example, setting the fractional unc. control to 0.1 indicates that near any f, 68% of the $P_V(f)$ data points should vary by $\pm$10 percent. Setting the reject control to 3 would then throw out (set the weights to zero) any points more than 30% "off." But off from what?

The program uses the fit as the baseline for the rejection. For the example, any points more than 30% from the current estimate of the fitted curve would be thrown out. The initial guess parameters define the current estimate of the fitted $P_V(f)$ according to Eq. 32, and they must be set close enough that good points are not tossed. Click on the show guess button to see the current estimate of the fitted $P_V(f)$ and the resulting rejected points, which are shown with overlying $\times$'s. Clicking on the do fit button initiates a round of nonlinear regression iterations using the included points. After the fitting routine returns, click on the copy button to transfer the ending parameter values from the fit to the initial guess parameters and display the new points that would be rejected in another round of fitting. Continue clicking the copy and then the do fit buttons until there are no further changes in the fit. Look carefully at the final excluded points to make sure valid points are not being rejected. Adjust the fractional unc. control to get a reduced chi-square around one (so that the parameter covariance matrix comes out approximately correct) and adjust the reject control so that only undesired points are rejected for the final fit.

$P_V(f)$ varies over several orders of magnitude and the fact that the fractional uncertainty is roughly constant over a wide range, indicates even the points out in the tails of the Lorentzian contain statistically significant information. If an equally weighted fit were used, the points in the tails would not contribute to the parameters as their contribution to the chi-square would be too small compared to the points at lower frequencies where $P_V(f)$ is much larger. Consequently, the fit should not be equally weighted. Because the data point y-uncertainties σ_i are proportional to y_i, the fit uses weights $1/\sigma_i^2$ proportional to $1/y_i^2$.

Raster Scan program

This program is used to scan the x- and y-piezos in a slow scan mode while averaging the signals from the QPD. Starting with a fixed voltage to the y-piezo, the x-piezo is scanned

over a user-defined range. Then the y-piezo is moved a small amount in one direction and the x-piezo is again scanned over that range. This is continued until the y-piezo has scanned over the user defined range. At each xy value, the program digitizes the V_x and V_y signals from the QPD module and displays the results for these signal as an intensity plot, with the ability to see one dimensional plots of the two signals in slices at constant x or constant y.

This program is currently only used for a check on the detector constant β for comparison with the value determined from the fit to the PSD.

General concerns

In addition to laser safety issues, please take care to observe the following precautions

- *Alignment of the optical system:* All optical elements have already been carefully aligned and optimized. The only optical adjustments you will need to make involve the focus and the positioning of the xyz stage using the manual controls on the stage. **Do not attempt to move, disassemble or adjust the optical fiber or any of the mirrors and lenses and other optical components.** If you disturb the laser alignment, the optical trap will cease to function and it will require tedious and time-consuming realignment. Any disassembly of the apparatus could also lead to accidental and very dangerous eye exposure to the laser beam.

- *The 100× objective:* Please take care that nothing (except immersion oil and lens paper) ever touches the lens of the lower microscope objective. In focusing or adjusting the stage you should not crash or scrape the slide against the lens. When you are finished for the day, please take a single sheet of lens paper and gently wipe the immersion oil from the lens. Do not scrub the lens: a single wipe with the paper is fine.

- *The laser optical fiber:* Please do not touch or handle the optical fiber. It is extremely delicate and costly to repair.

- *The laser settings:* The laser beam power (via the laser diode current) is adjustable, up to a maximum setting (upper limit value) that has been programmed into the laser power supply. The laser also has a thermostat controller that has been programmed to maintain the laser at its optimum temperature. You are welcome to adjust the laser current up to the maximum limit value, but please do not attempt to change the maximum limit value or the laser control temperature.

Procedures

Initialization

Turn on the power supply for the controller hub. Wait a few seconds for their firmware to initialize and then run the Initialize program. This program sets up all the T-Cube modules to run in the appropriate modes used in other programs. It sets the piezo and strain gauge feedback channel, zeros the piezos' outputs and then zeros the strain gauges. Finally, it sets the x and y piezos near their midpoint voltages of 37.5 V, and sets the operating mode to add this 37.5 V to the voltages generated by signals applied to the external input. In this way, the piezo is near the middle of its extension, and so both positive and negative translation in x and y can be generated by supplying positive or negative control voltages.

Be sure to turn off power supply to the controller hub before leaving the apparatus overnight. Voltages left on the piezos over long times can change their properties.

Motion calibration

Install the reticle slide on the sample stage with the calibration markings facing downward. Place a single small droplet of immersion oil onto the lower (100×) objective. (A small droplet of oil will remain on the lens and not run significantly.) Then using the stage z control *carefully* lower the slide down into proximity to the lens. Check the video camera and watch for the reticle image to come into focus. You will need to get the slide quite close to the objective lens (within a mm or so) to get into focus.

The first thing you need to do is determine the pixel calibration constant: How many microns correspond to one image pixel on the camera? Use the camera software measuring tool to determine the separation in pixels of known lengths on the reticle slide. Our camera pixels are square and you should find the same values in the x- and y directions. Determine the camera calibration constant in μm/pixel. Be sure to make several measurements so that you have an idea of your experimental precision.

Next use the x and y manual micrometers on the stage to determine their sensitivity. The micrometers have both coarse and fine (differential) operation, and one or the other will be in effect depending on how far you turn them. Learn when and how they switch sensitivity. The micrometer barrels are marked with 50 m-units (units on the main rotating sleeve) per rotation. Use the camera and reticule markings to determine the fine-control m-units per distance moved. This calibration constant is not far from 1 m-units per μm of real motion.

You must also determine motion calibrations involving the use of the piezo controls on the stage. There are separate piezo driver modules for each of the three axes—x, y and z. They can be used with or without strain-gauge feedback. To do a piezo calibration requires observing a silica bead stuck to a slide so that it will move with the slide and therefore with the stage. Find or make a new slide of stuck beads. They are made by diluting our stock beads in a 1% NaCl solution, which makes them stick to the slide. Try either the 1.2 or 1.5 μm beads. If a "stuck-sphere" slide dries out, it can be refreshed by refilling the channel with distilled water.

Beads diluted in a 1% detergent solution are used when you want to keep spheres from sticking to the slide or to each other.

The piezo motion with strain gauge feedback is used in the raster scan program. Learn how to run the raster scan program. To calibrate the piezo for this mode, set up a test from the raster program, measure the actual displacements with the camera and its pixel calibration constant and determine the real distance moved per percent of full scale.

Use the pixel calibration above with the plots on V_x and V_y versus % full scale piezo motion to determine the detector calibration constant β. Check it at a few different focusing positions, i.e., at the best focus and then slightly above and slightly below this z-position to see how small changes in the beads z-position relative to the laser focus affects β.

Adjusting the piezos with the strain gauge feedback cannot always be done fast enough—particularly when applying an oscillatory motion to the stage. In this case, the computer's two DACs (digital to analog converters) will be used to apply voltages directly to the input of the x and y piezo modules. The piezo module amplifies those voltages by about 7.5, adds

them to the 37.5 V offset and sends them on to the actual piezo-transducers in the stage. The DAC is then programmed for an oscillatory output of known amplitude and frequency and the resulting piezo motion will then be observed on the camera image. The camera's pixel calibration from the previous step is then used to determine the piezo calibration constant.

The direct DAC method of driving the piezo is used in the calibration program to determine the trap constants. For this calibration step, it will only be used to apply sinusoidal voltages that will drive oscillations in the stage position.

When hysteresis in the piezo is taken into account, an applied sinusoidal voltage of amplitude $V_{\rm DAC}$ will cause nearly sinusoidal oscillations of the position with an amplitude A that depends nonlinearly on $V_{\rm DAC}$. Run the "Oscillate Piezo" program while viewing a stuck sphere. With the $V_{\rm DAC}$ at zero, the piezo doesn't move and the amplitude of the stage motion is zero. As $V_{\rm DAC}$ increases, the motion amplitude increases with a quadratic dependence.

$$A = a_1 V_{\rm DAC} + a_2 V_{\rm DAC}^2 \qquad (34)$$

There can also be phase shifts between the motion oscillations and those of the driving voltage. These phase shifts will not need to be determined.

If the Oscillate Piezo program is made to apply equal amplitude oscillations to both the x and y piezos 90° out of phase with one another, this should drive the stage in a circle with a radius given by Eq. 34. Or you can set the x- or y-oscillation amplitude to zero so that the stage moves back and forth in one dimension. Use either method and measure A versus $V_{\rm DAC}$ in the range from 1 to 4.5 V and fit to Eq. 34 to determine a_1 and a_2. Check the relationship and several oscillation frequencies, up to 40 Hz. At higher frequencies, the stage accelerations for a given amplitude are larger and the stage inertia can affect this calibration. When measuring the PSD for particles in the trap, the stage oscillations will be in the 10-30 Hz range.

Sample sphere preparation

You will first need to prepare a sample of 1 μm silica microspheres. Since you will need to make measurements on a single sphere, getting their concentration correct is very important. Too few and it will be difficult to find any spheres. Too many and other spheres will likely wander into the trap and ruin the measurement. Use the pipettor to prepare approximately one ml of a 1000× dilution of the 1 μm microsphere stock in water. Load the diluted solution into a clean Ibidi microchannel slide with the 100 μm deep channel.

Be sure to use the vortex mixer just before sampling from the stock solution and also just before loading your diluted solution into the slide. The spheres tend to settle and the vortex mixer is needed to get them uniformly distributed in the suspending liquid. If you do not mix, the density of spheres will be wrong. Moreover, if you don't mix the main stock solution before taking a sample, you would be changing the concentration of the remaining stock solution.

The Ibidi slide has wells on each side where the solution is introduced. Put about 100 μl or so in one well and use a syringe to suck it through the channel, taking care not to suck air into the channel. (Add another 50 μl as the well empties.) It is easier to see the liquid coming into the channel if the slide is placed on a dark background. When filled, add or remove the solution to the wells as necessary to get it equally high in each well. If the heights are unequal, there will be a pressure differ-

ence which will drive the fluid from one well to the other until the pressure difference is eliminated. Even if you get the well heights equal by eye, small differences can still drive the fluid and it can take 10-15 minutes for the motion to cease. It can be very difficult to see spheres if they are moving with any but the smallest velocity flow.

Make sure the infrared laser is OFF and the LED light source is ON. Place a single small droplet of immersion oil onto the lower ($100\times$) objective. Then mount your Ibidi slide onto the microscope stage and *carefully* slide the stage into position over the lens, watching that you do not crash the slide into the objective: the bottom of the Ibidi slide should be above the objective lens. Then using the manual z micrometer *carefully* lower the slide down into proximity to the lens. As with the reticle slide, watch the video image for the sample to come into focus. Note that by adjusting the z-control you can scan the focus from the bottom to the top of the fluid channel.

Watch for individual spheres to become visible on the video monitor. When you see spheres, turn on the laser current to approximately 300 mA. By moving the stage you should be able to capture a particle into the trap. You will know that a particle is trapped because it will remain in the same location and same focus, even as you adjust the stage from side to side (xy) as well as up and down (z). Mark the trap position on the video image with the circle tool on the camera software. You can save the overlaid drawn circle and other drawn lines with the x|y menu item.

If you are observing a particle trapped in the z-direction, its focus will not change when you adjust the stage up and down in the z-direction. While you are moving the slide, the trapped particle's position is fixed because the laser focus is fixed relative to the $100\times$ objective If you raise the slide enough, however, sooner or later the sphere will hit the bottom of the 100 μm-deep channel in the slide and then go out of focus if you continue raising the slide. Similarly, if you lower the slide enough, the sphere will hit the top of the channel. If the trap is weak, you may have problems keeping a sphere trapped near the top of the channel. Because of the optical properties of the objective and sample, the trap force in the z-direction is expected to weaken as the sphere height increases.

See if you can use the micrometer calibration to demonstrate a trapped sphere can move from top to bottom of the channel. Then be sure to make measurements at lest 20 μm from the bottom of the channel. Viscosity effects cause the motion of the liquid around the spheres to change when the spheres are close to the bottom or top surface of the channel. Beyond 20 μm or so, the surfaces are effectively infinitely far away as far as viscosity effects go.

Steps: Experiment with capturing and manipulating silica spheres. Operate the LabVIEW Laser Tweezers software. Set the x and y V_{DAC} amplitudes for stage oscillations to zero. Set the acquisition and timing parameters. Begin acquiring the QPD signal and averaging the calculated PSD $P_V(f_j)$. When it is sufficiently smooth, stop the averaging, switch over to the Fit tab and do a fit of the PSD to Eq. 32.

Turn on the piezo oscillation of the stage and set the $V_{\rm DAC}$ that would give a stage oscillation amplitude $A = 0.1 - 0.3$ μm. Begin averaging the PSD and perform a full analysis to determine β, γ and k. Repeat at different laser powers. Plot the trap strength k, the calibration constant β, and the drag coefficient γ as a function of laser current. Discuss.

Repeat for a second silica particle size.

Prepare a dilute culture of *E. coli*. Capture a dead bacterium and use the calibration program to determine the trap force. Then

trap a swimming bacterium. Lower the laser power until it swims free. How well can you determine the swimming force generated by the bacterium from this measurement? With the laser off, watch a swimming bacterium and determine their typical speeds. Estimate the size of the bacteria. Its *hydrodynamic radius* is that value of a that gives the actual drag force $F_d = -\gamma v$ when the Einstein-Stokes formula (Eq. 3) is used with that a. Compare the two force determinations. Use your measurements to estimate the power generated by the flagellar motor of the swimming bacterium.